Chemie der Erde 75 (2015) 273–285

Contents lists available at ScienceDirect

Chemie der Erde

journal homepage: www.elsevier.de/chemer

Invited review

Asteroid (4) Vesta II: Exploring a geologically and geochemically complex world with the Dawn Mission

Timothy J. McCoy[a,*], Andrew W. Beck[a,b], Thomas H. Prettyman[c], David W. Mittlefehldt[d]

[a] Department of Mineral Sciences, National Museum of Natural History, Smithsonian Institution, Washington, DC 20560-0119, USA
[b] Applied Physics Laboratory, The Johns Hopkins University, 11100 Johns Hopkins Road, Laurel, MD 20723, USA
[c] Planetary Science Institute, 1700 East Fort Lowell, Suite 106, Tucson, AZ 85719, USA
[d] Astromaterials Research Office, NASA Johnson Space Center, Mail code KR, Houston, TX 77058, USA

ARTICLE INFO

Article history:
Received 9 May 2014
Accepted 1 December 2014
Editorial handling - K. Keil

Keywords:
Asteroid
Craters
Impacts
Meteorites
Dawn mission

ABSTRACT

More than 200 years after its discovery, asteroid (4) Vesta is thought to be the parent body for the howardite, eucrite and diogenite (HED) meteorites. The Dawn spacecraft spent ~14 months in orbit around this largest, intact differentiated asteroid to study its internal structure, geology, mineralogy and chemistry. Carrying a suite of instruments that included two framing cameras, a visible-near infrared spectrometer, and a gamma-ray and neutron detector, coupled with radio tracking for gravity, Dawn revealed a geologically and geochemically complex world. A constrained core size of ~110–130 km radius is consistent with predictions based on differentiation models for the HED meteorite parent body. Hubble Space Telescope observations had already shown that Vesta is scarred by a south polar basin comparable in diameter to that of the asteroid itself. Dawn showed that the south polar Rheasilvia basin dominates the asteroid, with a central uplift that rivals the large shield volcanoes of the Solar System in height. An older basin, Veneneia, partially underlies Rheasilvia. A series of graben-like equatorial and northern troughs were created during these massive impact events 1–2 Ga ago. These events also resurfaced much of the southern hemisphere and exposed deeper-seated diogenitic lithologies. Although the mineralogy and geochemistry vary across the surface for rock-forming elements and minerals, the range is small, suggesting that impact processes have efficiently homogenized the surface of Vesta at scales observed by the instruments on the Dawn spacecraft. The distribution of hydrogen is correlated with surface age, which likely results from the admixture of exogenic carbonaceous chondrites with Vesta's basaltic surface. Clasts of such material are observed within the surficial howardite meteorites in our collections. Dawn significantly strengthened the link between (4) Vesta and the HED meteorites, but the pervasive mixing, lack of a convincing and widespread detection of olivine, and poorly-constrained lateral and vertical extents of units leaves unanswered the central question of whether Vesta once had a magma ocean. Dawn is continuing its mission to the presumed ice-rich asteroid (1) Ceres.

Published by Elsevier GmbH.

Contents

* Corresponding author. Tel.: +1 202 633 2206; fax: +1 202 357 2476.
E-mail address: mccoyt@si.edu (T.J. McCoy).

http://dx.doi.org/10.1016/j.chemer.2014.12.001
0009-2819/Published by Elsevier GmbH.

1. Introduction

Of all the processes that have shaped the rocky planets of the Solar System, none has been as critical as differentiation. Rocky planets and asteroids accreted from essentially cosmic sediments of mixed silicates, metal, sulfides and, in some cases, ice. These cosmic sediments are preserved as chondritic meteorites. Yet chondritic meteorites are unlike any rock found on any of the terrestrial planets. Melting, differentiation and gravitational segregation separated the disparate components of chondrites, producing the layered metallic core, ultramafic silicate mantle and mafic/silicic crust structure so well-known on Earth and present in the other rocky planets and some asteroids. Despite sitting at the top of such a layered structure, we still have an incomplete understanding of how this fundamental process first occurred in the earliest history of our planet. This stems in part from an incomplete sampling of the layers and in part from the subsequent processes – including impact, plate tectonics, and mixing between layers – that has followed over the past 4.56 Ga on Earth.

While Mercury, Venus, Earth and Mars all experienced dramatic geologic events subsequent to their initial differentiation, the same cannot be said of asteroids that melted and differentiated. With their high surface to volume ratio, they radiated heat effectively after melting and, hence, cooled quickly. In most cases, internal heating stopped within 100–150 Ma after the birth of the Solar System (Wadhwa et al., 2006). The only dominant process altering them since that earliest epoch has been impact bombardment. For this reason, asteroids serve as the ideal subjects to understand early Solar System differentiation. It was this logic that led the Dawn mission to explore asteroids (4) Vesta and (1) Ceres.

2. Asteroid (4) Vesta

On January 1, 1801, Giuseppe Piazzi first discovered an asteroid that would be rediscovered exactly one year later by Franz Xaver von Zach and named (1) Ceres. On March 29, 1807, H.M. Wilhelm Olbers discovered asteroid (4) Vesta (henceforth for simplicity referred to as Vesta), the last discovery of an asteroid for 38 years (Russell and Raymond, 2011). It was named for the virgin goddess of home, hearth and family from Roman mythology. As early as 1879, E.C. Pickering estimated the diameter of Vesta at 513 ± 17 km, close to the modern value, although subsequent measurements varied by nearly 100 km in diameter (Hughes, 1994). Bobrovnikoff (1929) discovered rotational color and albedo variations attributed to composition. In 1966, Vesta's gravitation perturbations of asteroid (197) Arete were used to estimate its mass (Hertz, 1968). Vesta is the second most massive asteroid, behind Ceres, and third in volume behind Pallas. Vesta was detected by radar by Ostro et al. (1980).

Interest in Vesta accelerated with the pioneering work of McCord et al. (1970), who showed that the spectral reflectance of Vesta was markedly similar to that of the basaltic eucrite Nuevo Laredo. Nuevo Laredo is a member of the howardite–eucrite–diogenite (henceforth HED) clan of meteorites, the largest group of achondrites (igneous stony meteorites) in our collections. For example, the HEDs comprise ~62% of the achondrites in the US Antarctic Meteorite Collection and provide ~50 kg of mass for laboratory study in that collection alone (Corrigan et al., 2014). If Vesta is indeed the parent body of the HED meteorites, our opportunities for simultaneous geologic, geophysical and geochemical exploration of this largest differentiated asteroid expand significantly. A compelling impediment to arguing for the linkage between HED meteorites and Vesta was the semi-major axis of Vesta at 2.36 AU, far from the preferred meteorite delivery locations in the 3:1 resonance (where an asteroid would orbit three times for each orbit of Jupiter) at 2.5 AU or the ν_6 resonance (a perihelion secular resonance between asteroids and Saturn). This objection was nullified by Binzel and Xu (1993), who observed smaller asteroids that were spectrally and dynamically linked to Vesta – the vestoids – between the 2.36 AU orbit of Vesta and the 2.5 AU 3:1 resonance. It is these smaller asteroids that provide a path for the meteorites. The likely source of the vestoids was revealed by Thomas et al. (1997) based on Hubble Space Telescope (HST) observations of Vesta in 1996 (Fig. 1). These authors fit Vesta's shape with an ellipsoid of 289 by 280 by 229 km, yielding densities (using a known range of masses) of 3.5–3.9 g/cm^3. Further, these authors discovered on the asteroid an ~460 km diameter crater (now named Rheasilvia, after the mother of Romulus and Remus, the legendary founders of Rome) at the south pole, with a total relief of ~24 km, and color measurements consistent with excavation of a high-calcium, pyroxene-rich crust or olivine-rich upper mantle within this impact crater.

It is particularly interesting to consider the difference between mankind's exploration of the Moon and asteroid Vesta. For more than four centuries, humans have trained telescopes at the Moon and naked eye observations of the Moon were conducted for

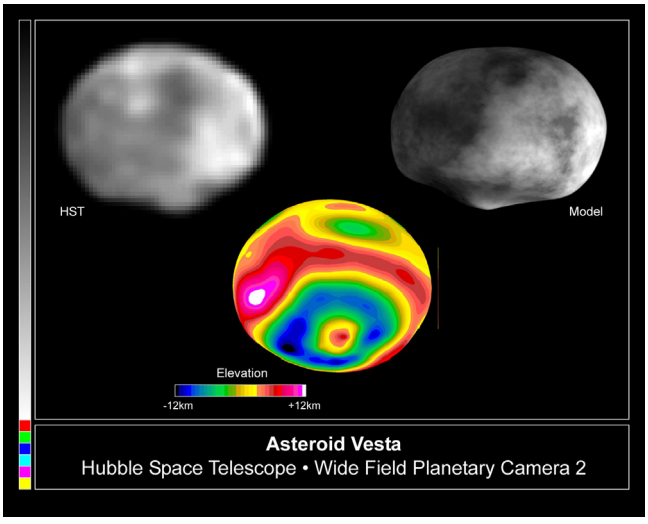

Fig. 1. Composite image of Hubble Space Telescope image. At top left is a Hubble Space Telescope image of Vesta. At top right is a digital shape model. Both images exhibit a prominent projection at the flattened south pole, which is interpreted as the central uplift of a large basin. Shading on the digital shape model is artificial and not indicative of albedo differences. Bottom center is a dynamic height solution projected onto Vesta's shape model and viewed from 33°S. Image courtesy of Ben Zellner (Georgia Southern University), Peter Thomas (Cornell University) and NASA.

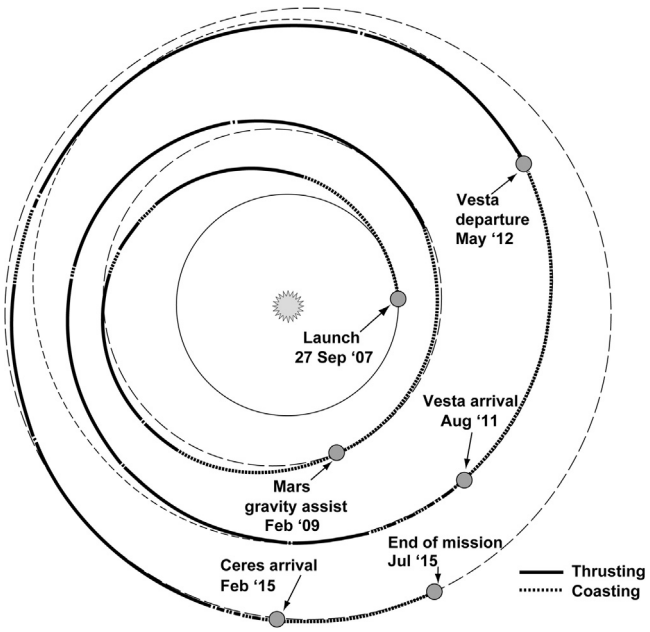

Fig. 2. Dawn mission trajectory from launch on Sept. 27, 2007 through to arrival at Ceres nominally in the Spring of 2015. Note that the unique ion propulsion system is thrusting during the majority of the transit, with intermittent periods of coasting. Image courtesy of JPL.

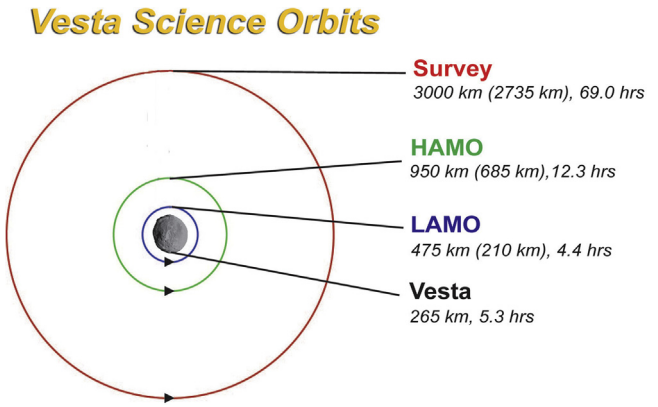

Fig. 3. Three science orbits were established around Vesta, each driven by a different science instrument. Altitudes for the orbits listed are from the center of Vesta and in parentheses above the surface of the 265 km diameter asteroid. The visible-infrared spectrometer was prime driver during Survey orbit, while framing camera controlled during the high-altitude mapping orbit (HAMO) and the gamma ray and neutron detector (GRaND) controlled during the low-altitude mapping orbit (LAMO). The spacecraft entered HAMO both during descent to the asteroid and ascent, resulting in HAMO-1 and HAMO-2 phases. Image courtesy of UCLA/McREL.

millennia before the telescope. By the time of the first lunar landings, our knowledge of the geology and topography of the Moon was reasonably advanced. The return of ~382 kg of lunar samples by the Apollo and Luna missions added detailed geochemical, geological, petrological and chronological knowledge to our history of the Moon, ultimately allowing us to derive the origin and evolution of our nearest neighbor. Our exploration of Vesta differed drastically from that of the Moon, with the acquisition of samples before imaging. We had already sampled more than 1000 kg of HED meteorites thought to originate from Vesta before obtaining the high-resolution images necessary to provide geologic context for these precious samples. Indeed, a detailed interpretation of the HED parent object was developed eight years prior to identification of the spectral match between Vesta and Nuevo Laredo, when Mason (1962) suggested that the major types of meteorites were related by fractional crystallization, presaging the magma ocean model.

Pre-Dawn observations set the stage for exploration of an ancient differentiated body from which we have abundant samples by which to both derive models of the asteroid and compare remote observations. There was also the considerable promise that the interior of the asteroid might be revealed within the Rheasilvia impact basin.

3. Spacecraft and mission profile

Detailed descriptions of the Dawn mission, including pre-mission knowledge of the target asteroids, history of the mission, details of the mission profile, and descriptions of the major systems and subsystems, including the instruments, are given in a special issue of *Space Science Reviews* (2011, Vol. 163, Issues 1–4). We reiterate selected, abbreviated portions of these papers in this section. Selected within NASA's Discovery Program of low-cost missions in 2001, Dawn is a joint project of Orbital Sciences Corporation and the Jet Propulsion Laboratory (Russell and Raymond, 2011). Dawn was launched on Sept. 27, 2007 from Cape Canaveral Air Station, following an outwardly spiraling trajectory with interspersed periods of thrusting with the ion propulsion engines and coasting (Fig. 2). On Feb. 17, 2009, Dawn passed 543 km above the surface of Mars to achieve a gravity assist to reach Vesta. As it approached Vesta, Dawn had three rotational characterization phases at spacecraft-asteroid distances from 100,000 to 5200 km and spatial resolutions of ~9000 to ~500 m/pixel. With its novel propulsion system (discussed below), Dawn was gently captured by the gravity of Vesta on July 15, 2011 U.S. Pacific Time. Once in orbit, Dawn employed three circular, polar orbits – the Survey orbit at 3000 km (average orbital distance) from the center of Vesta, the High Altitude Mapping Orbit (HAMO) at 950 km, and the Low Altitude Mapping Orbit (LAMO) at 465 km (Fig. 3). These three orbital phases benefit the scientific payload on Dawn in various ways, discussed below. After reaching Survey orbit and descending through HAMO to LAMO, Dawn then reversed the process to reach HAMO-2 before escaping the gravity of Vesta on Sept. 5, 2012 U.S. Pacific Time. Dawn's last mission phase was a fourth rotational characterization. Dawn is currently enroute to asteroid 1Ceres with an estimated arrival in late March or early April 2015.

The Dawn spacecraft is based on the STARBus geosynchronous configuration, with a cube surrounding a central cylinder that houses the electronics and propulsion systems (Thomas et al., 2011) (Fig. 4). The spacecraft had a dry mass of 747 kg and carried 45.5 kg of hydrazine for the reaction control system and 425.3 kg of xenon for the ion propulsion system. The three science instruments are all mounted in the +*Z* direction and co-aligned. Two of the more remarkable features of the spacecraft design are the solar panels and the ion propulsion system. Providing sufficient electrical energy to operate the electric ion propulsion system and to provide power to the other systems is a significant challenge for a solar-powered spacecraft operating at 3 AU. To provide the needed power, the spacecraft carries fixed on each side 5-panel solar "wings" that each measure 2.27 by 8.3 m. When fully extended, the two solar panels give the spacecraft an overall length of 19.73 m. The ion propulsion system (Brophy, 2011) operates by ionizing onboard xenon, which is then electrostatically accelerated to speeds as high as 40 km/s. Amazingly, the thruster produces a force of 18.8–91.0 mN, comparable to the force exerted by a single sheet of US letter or A4 paper pushing on the palm of your hand in Earth's gravity (~50 mN). Unlike standard rocket propulsion, intervals of continuous thrusting can last for weeks or months. Without standard rocket propulsion, the spacecraft also doesn't execute burns during critical maneuvers. The most interesting consequence of this is that no orbital insertion maneuver was executed

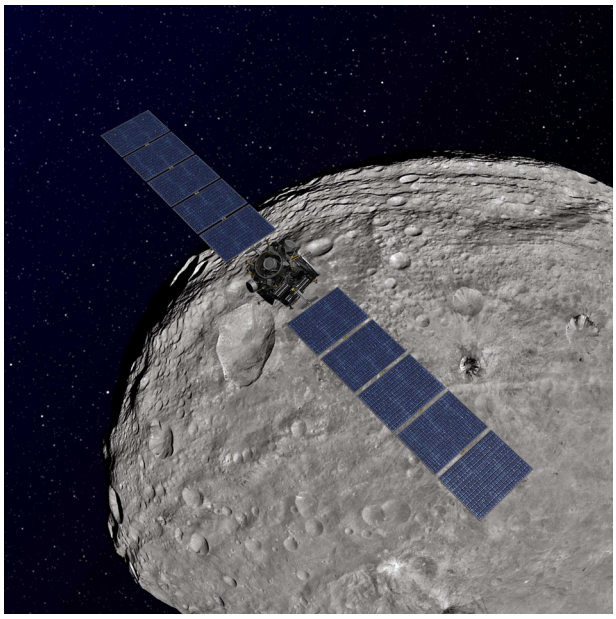

Fig. 4. Artist's concept of the Dawn spacecraft superimposed on an image of asteroid Vesta. The solar panels on the spacecraft span a total of 19.73 m. Such large solar panels are necessary to provide sufficient electrical energy to the ion propulsion engine at heliocentric distances of 3 AU while operating in the main asteroid belt. Image courtesy of NASA/JPL-Caltech.

to place Dawn into orbit around Vesta. Instead, the asteroid simply captured the spacecraft into its gravitational well.

Dawn carries three instruments—framing cameras (FC) (Sierks et al., 2011), a visible and infrared mapping spectrometer (VIR) (De Sanctis et al., 2011) and a gamma ray and neutron detector (GRaND) (Prettyman et al., 2011) (Fig. 5). The framing camera covers the wavelength range from 0.4 to 1.0 μm with seven color and one clear filter at resolutions down to ~17 m/pixel for LAMO images. Images from the framing camera are used for global shape, local topography and surface geomorphology, and reflectance measurements. FC filter selection allows for a relative estimate of the 1 μm absorption feature and the spectral slope. VIR, the primary mineral mapping instrument on Dawn, is a hyperspectral spectrometer with imaging capabilities. VIR provides mineral identification by combining a visible channel from 0.25 to 1.05 μm and an infrared channel from 1 to 5.0 μm with spatial resolution down to <60 m/pixel in LAMO. Given the dominance of minerals in the HED group with strong absorption features in the 1–2.5 μm range (De Sanctis et al., 2011), VIR is essential in mapping the distribution of HED lithologies on Vesta. The GRaND spectrometer measures gamma-rays along with thermal, epithermal and fast neutrons emitted from the upper meter of the regolith on Vesta. These nuclear emissions result from the decay of radioelements and nuclear reactions induced by galactic cosmic rays, which steadily bombard Vesta's surface. The spectrum of gamma rays and neutrons provides a fingerprint that can be analyzed to determine the elemental composition of Vesta's regolith to depths of a few decimeters Prettyman et al. (2011). In LAMO, GRaND was able to resolve regional-scale spatial variations (about 300 km) in elemental composition, including the abundance of hydrogen. Finally, the navigation system also allows Dawn to undertake gravity investigations at Vesta and Ceres.

Different spatial resolution of the instruments onboard Dawn led to varied scientific benefits for each instrument during the three orbital stages. The spatial resolution of FC and VIR ranged from ~250 to 20 and ~700 to 70 m/pixel, respectively, across the three orbital stages. These instruments provided data during each orbital stage; however they were the main science drivers during Survey and HAMO. GRaND was primarily utilized during the LAMO stage, where it achieved a spatial resolution of about 300 km/pixel.

4. Vesta's shape, internal structure, and surface morphology

4.1. Size, density and the core

Upon arrival and spiraling down into the survey orbit, the Dawn mission mapped ~80% of the surface of Vesta. Dawn arrived during northern winter; however, as the mission progressed a greater portion of the northern surface was illuminating allowing nearly full coverage of the surface with Dawn's optical instruments. The northern polar region was not illuminated, owing to the obliquity of the asteroid. Dawn's early observations were summarized in a series of papers by Russell et al. (2012), Jaumann et al. (2012), Marchi et al. (2012) and Schenk et al. (2012), and we summarize these observations here and in the next section.

The shape model allowed determination of a best fit ellipsoid of 286.3 by 278.6 by 223.2 km with an uncertainty of ±0.1 km, slightly outside the previous estimate of 280 by 289 by 229 km with a stated uncertainty of ± 5 km (Russell et al., 2012). The refined volume, coupled with a mass of 2.59076×10^{20} kg, yields a density of 3456 kg/m^3. This value is at the low end of previous estimates for Vesta (3500–3900 kg/m^3) and lower than grain densities for ordinary chondrite falls (3540–3720 kg/m^3; Consolmagno et al., 1998), but similar to the bulk density of H chondrites (3420 kg/m^3). However, the new density is well above densities reported for smaller asteroids (e.g., 433 Eros at 2670 kg/m^3) which contain significant macroporosity. The relatively high density of Vesta suggests that it contains considerably less macroporosity than smaller asteroids, many of which are fragments formed by catastrophic fragmentation of larger original asteroids. Such a relatively high density also has implications for the presence and size of a core in this almost intact protoplanet.

Constraints on the size of Vesta's core prior to Dawn have come exclusively from modeling partitioning of siderophile elements between the rocky mantle and crust and the core (Zuber et al., 2011). The earliest estimate of the mass of the core of Vesta, relative to the asteroid as a whole, were in the range of 40–50% (Newsom, 1985). Later estimates using revised partition coefficients and a range of potential starting compositions yield core masses between 5 and 25%. Ruzicka et al. (1997) argued for a best estimate of the mass of the core at 5%, with an upper limit of <30%. For a range of 5–25% mass of metal, the core radius would range between 75 and 128 km. The most recent modeling by Toplis et al. (2013) for a range of chondritic precursors suggests core radius in the range of 100–120 km, although bulk core densities range from ~5000 to 8000 kg/m^3, essentially from almost pure sulfide to pure metal compositions. These authors note that a Na-depleted H-chondrite bulk composition can match many of the geochemical features consistent with the petrogenesis of the HED clan of meteorites, but oxygen isotopes and oxidation state may require admixture of 25% of a CM-like component. Such a mixture of 75% H chondrite and 25% CM chondrite yields a core radius of 114 km.

The derived density for Vesta combined with the gravitation moment obtained from gravitational tracking can constrain models for Vesta's interior consistent with geophysical and geochemical constraints (Russell et al., 2012). Using a simplified two-layer mass balance model and a range of core densities consistent with iron meteorites (7100 and 7800 kg/m^3), these authors derived an average core size of 107–113 km, equivalent to a core mass fraction of ~18%, within the range of values derived by Righter and Drake (1997) and Ruzicka et al. (1997). However, the range of uncertainty cited is almost certainly too low given the unknown density

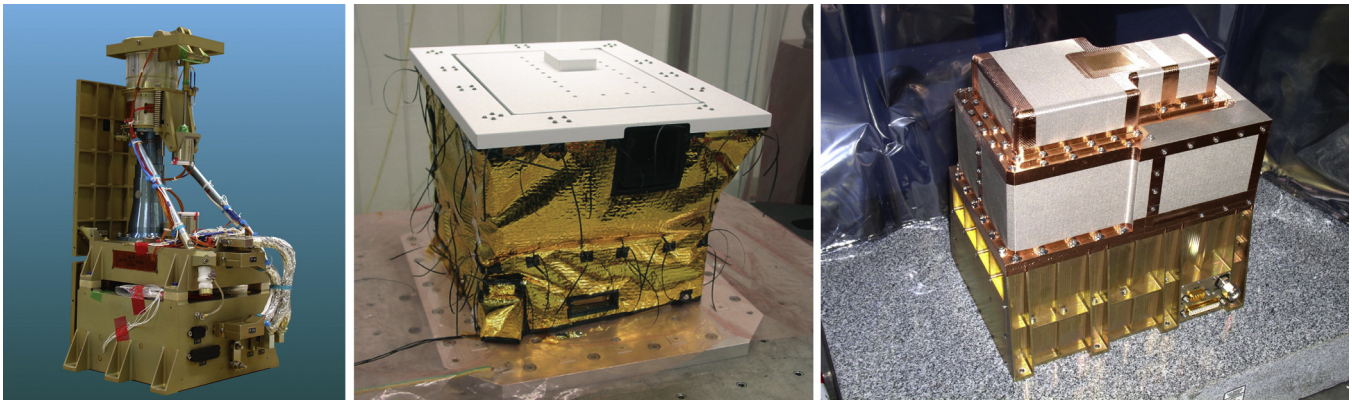

Fig. 5. Dawn carries three instruments. The framing camera (left) covers 0.4 to 1.0 μm with one clear and seven color filters. The Dawn spectrometer (VIR) (center) is a hyperspectral spectrometer (0.25–5.0 μm) with imaging capabilities. The GRaND spectrometer (right) measures gamma-ray and thermal and epithermal neutrons in the upper meter of the regolith to infer regional-scale composition. *Note*: images not to scale. Images courtesy of MPS, SELEX GALILEO-ASI-INAF and Los Alamos National Laboratory, respectively.

of the core, assumptions about a 2-layer structure, and effect of macroporosity. Toplis et al. (2013) suggest a core radius for a core with higher sulfur contents in the range of ~115 km (~15% core mass fraction), and that estimate could range to ~130 km. Despite the uncertainties, the Dawn estimate for the radius of the core of Vesta is broadly consistent with pre- and post-mission modeling of extensive differentiation of Vesta starting from a range of likely chondritic precursors, supporting the idea of extensive melting and near-complete segregation of metal to the core.

4.2. Craters, mountains and troughs

The existence of a south polar basin on Vesta created tremendous anticipation for the first images of the asteroid. While still 189,000 km away, Dawn's framing camera captured images with better than twice the resolution of those taken by the Hubble Space Telescope (HST) in 1997 (http://dawn.jpl.nasa.gov/feature_stories/dawn_vesta_062011_full_description.asp). By early July 2011, at distances in excess of 40,000 km from Vesta, Dawn's framing camera began to provide detailed images that would redefine our understanding of the surface of the largest asteroid visited to date.

The most dramatic feature revealed in the earliest images was the central uplift of the south pole basin Rheasilvia (Fig. 6) (Schenk et al., 2012). Created by rebound of the underlying rock after peak compression during crater formation, central uplifts are a common feature of large impact basins on the Earth, Moon, Mars and Mercury, as well as on the satellites of the outer planets. As noted by Schenk et al. (2012), the dimensions of Rheasilvia are similar to that observed on the midsize icy satellites Hyperion, Rhea, and Iapetus. These authors suggested that the basic morphology of a large central uplift dominating over rim collapse and multi-ring basin formation may be characteristic of low-gravity bodies. During the survey orbit at ~2700 km altitude, stereophotogrammetric analysis revealed an overall relief from −22.3 to 19.1 km, which slightly exceeds the relief indicated by HST images (−25.4 to 13.7 km). As expected, a large area of low relief was observed near the south pole of Vesta. When recast to a projection centered on the south pole (Fig. 7), the scale and relief of the Rheasilvia basin become obvious.

At ~500 km in diameter and ~19 km deep (Schenk et al., 2012), Rheasilvia is among the largest basins relative to the diameter of the planetary body in the Solar System. With nearly 20 km of vertical relief, the central uplift in the Rheasilvia basin stands as the second highest mountain in the Solar System, significantly exceeding the Hawaiian shield volcanoes and trailing only the massive Olympus

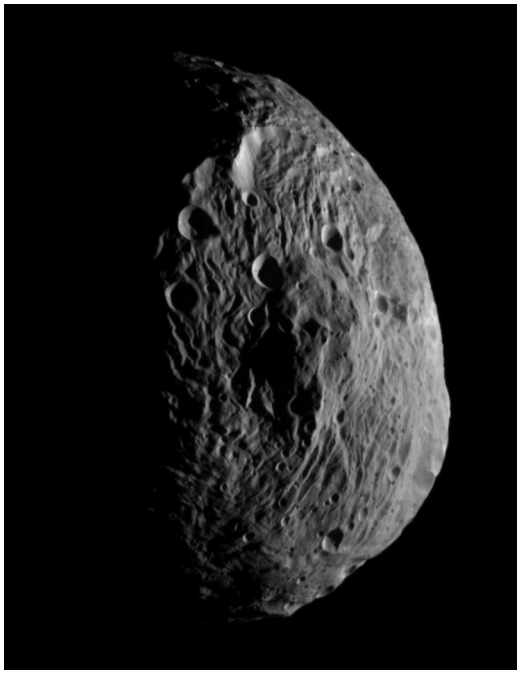

Fig. 6. Image of Vesta captured by the framing camera on Dawn on 18 July 2011 at a distance of 10,500 km. In the center of the image is the dramatic central uplift almost centered at the south pole of Vesta in the center of the Rheasilvia basin. Image courtesy of NASA/JPL-Caltech/UCLA/MPS/DLR/IDA.

Mons shield volcano on Mars. It is remarkable that the Rheasilvia central peak formed not through convergent plate tectonics or hot-spot volcanism, as did the other great mountains of the Solar System, but through rebound during crater formation. Two arcuate scarps ~5–7 km high on the central uplift suggest partial collapse. Collapse features are also observed along the edges of the Rheasilvia basin, where scarps ~15–20 km high have slump blocks at their base consistent with collapse.

While the existence of a single south pole basin had been inferred from HST images, topographic maps of Vesta revealed a second basin, named Veneneia (Fig. 7) after one of the founding vestal virgins. Veneneia is ~400 km in diameter and ~12 km deep. Rheasilvia is superimposed upon Veneneia and destroys about half of the older structure. Crater counts of the floors of these two large basins suggests ages of ~1 Ga for Rheasiliva and ~2 Ga for Veneneia (Schenk et al., 2012). In addition to these two large basins, at least

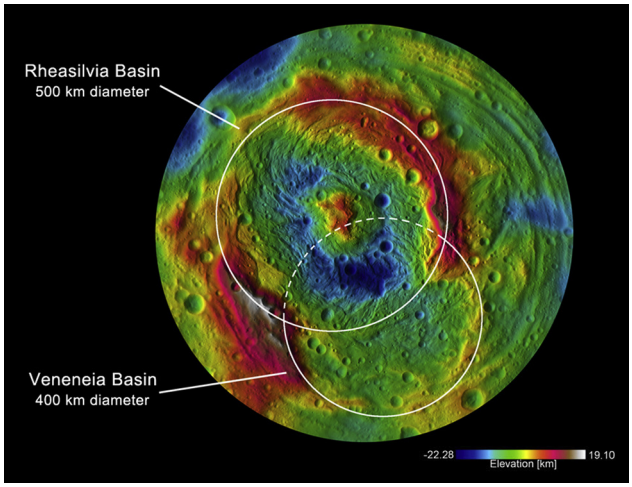

Fig. 7. Color-coded topographic map of Vesta illustrating the superposition of Rheasilvia, which dates to ~1 Ga, over the Veneneia basin, which dates to ~2 Ga. Image courtesy of NASA/JPL-Caltech/UCLA/MPS/DLR/IDA. (For interpretation of the references to color in this figure legend, the reader is referred to the web version of this article.)

10 other craters on Vesta exceed 50 km in diameter (Fig. 8), including an older, ~250 km diameter crater that is also superimposed by Rheasilvia. A general paucity of craters in the south is consistent with resurfacing of much of Vesta by Rheasiliva and Veneneia, while heavily cratered terrains in the north appear to be old, stable surfaces that escaped resurfacing by ejecta from these southern basins. O'Brien et al. (2014) argued that the northern heavily cratered terrain could date to 4.3–4.5 Ga, while supporting an age of ~1 Ga for Rheasilvia.

A second unexpected feature of Vesta is the presence of equatorial and northern ridges and troughs (Jaumann et al., 2012). The primary set of equatorial troughs are wide, flat-floored and bounded by steep scarps, with lengths varying from 19 to 380 km and up to 15 km in width. In contrast, northern troughs are offset from the equatorial troughs by about 30° and reach lengths up to 390 km and widths up to 38 km. The features of the northern troughs are more muted, suggesting an older age of formation. Fitting planes to the two sets of troughs and determining a pole perpendicular to the center of the plane yields pole directions that are, within error, at the center of the Rheasilvia basin for the equatorial troughs and Veneneia for the northern troughs (Fig. 9). This strongly suggests that the troughs formed as a result of impact deformation during the formation of these basins. Buczkowski et al. (2012) suggest that these troughs are graben and their formation is limited to differentiated bodies, of which Vesta is the smallest, intact differentiated body known in the Solar System.

5. Vesta's surface composition

5.1. Observations from FC images and VIR spectra: One big howardite

After the establishment of the Vesta/HED connection (McCord et al., 1970), and subsequent confirmation by the discovery of the vestoids (Binzel and Xu, 1993), many HED meteorite studies focused on predicting petrologic models for the formation and evolution of Vesta based on HED compositions (e.g., Mittlefehldt et al., 1998; McSween et al., 2011 and references therein). It was anticipated that data returned from the Dawn mission to Vesta would be used to test these models through the identification and mapping of igneous eucrite and diogenite lithologies on the surface of Vesta. This mapping was to be achieved by combining the high spatial resolution FC color data (Reddy et al., 2012a,b) with the high spectral resolution VIR data (De Sanctis et al., 2012), utilizing the strong 0.9 μm (BI) and 1.9 μm (BII) absorption features of pyroxene (Burns, 1993), a major component in all HED meteorites. Diogenites, which contain MgO-rich low-Ca pyroxene, have absorption features on the shorter side of BI and BII, at ~0.91 and ~1.88 μm, respectively (Gaffey, 1976). The more FeO-rich eucrites, which contain both high- and low-Ca pyroxene, have BI and BII features centered at longer wavelengths, ~0.95 and ~2.02 μm, respectively (Mayne et al., 2010). The relative abundance of high- and low-Ca pyroxene and, to a lesser extent, its FeO content in diogenites and eucrites leads to variations in the strength of the BI and BII features due to the change in crystal field site size (Burns, 1993); the low-Ca pyroxene-dominated diogenites have BI and BII depths of ~0.65 and ~0.42 (range in reflectance), while the high- and low-Ca pyroxene + plagioclase-bearing basaltic eucrites have shallower BI and BII depths of 0.42 and 0.24, respectively (De Sanctis et al., 2012). Being mixtures of eucrites and diogenites, the strength and center of howardite BI and BII absorption features form a continuum between the two igneous end members.

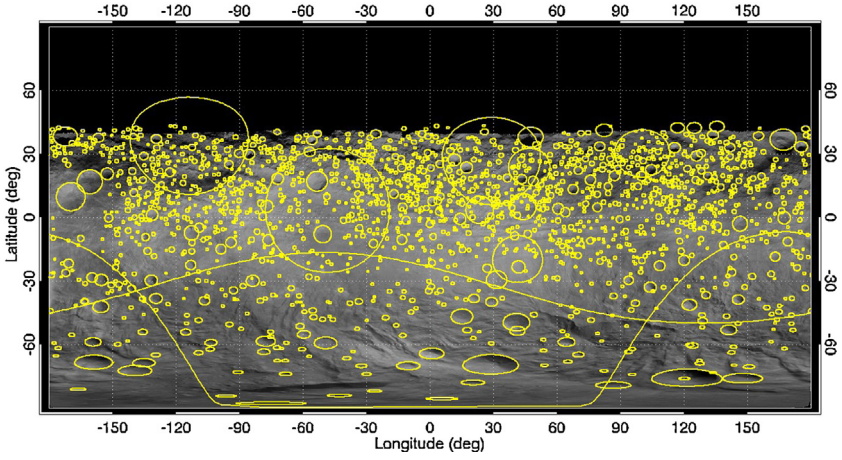

Fig. 8. Global distribution of craters on Vesta mapped from Dawn framing camera images. Yellow circles indicate craters of 4 km diameter or wider, with the size of the circles indicating the size of the crater. The two huge impacts in the southern hemisphere appear as undulating lines in this projection. A general paucity of craters in the south is consistent with resurfacing of Vesta from the Veneneia and Rheasilvia basins. Concentrations of craters around 30°N and 0 to −30 and 60–120 in longitude indicate particularly old terrains. Image courtesy of NASA/JPL-Caltech/MPS/DLR/IDA/PSI. (For interpretation of the references to color in this figure legend, the reader is referred to the web version of this article.)

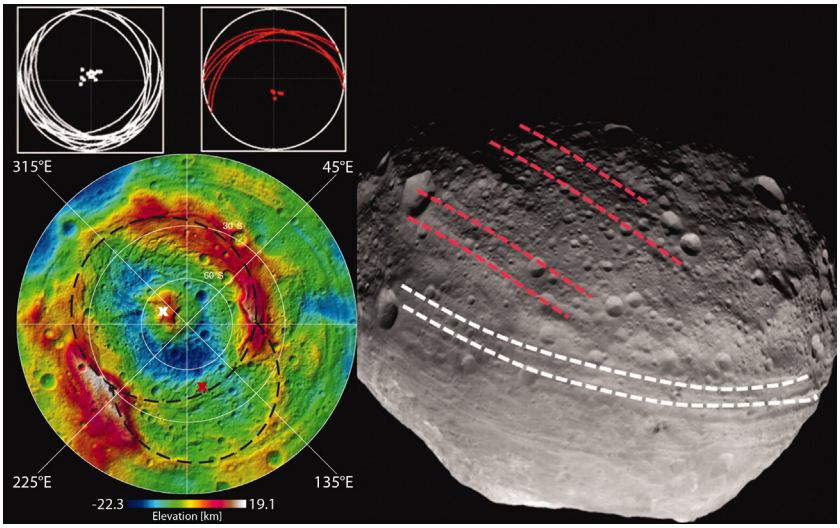

Fig. 9. Equatorial (white) and northern (red) troughs on Vesta. The center positions of the trough sets correspond to the center of Rheasilvia (white ×) and Veneneia (red ×), respectively. Reprinted with permission from Jaumann et al. (2012, Science 336, 687–690). (For interpretation of the references to color in this figure legend, the reader is referred to the web version of this article.)

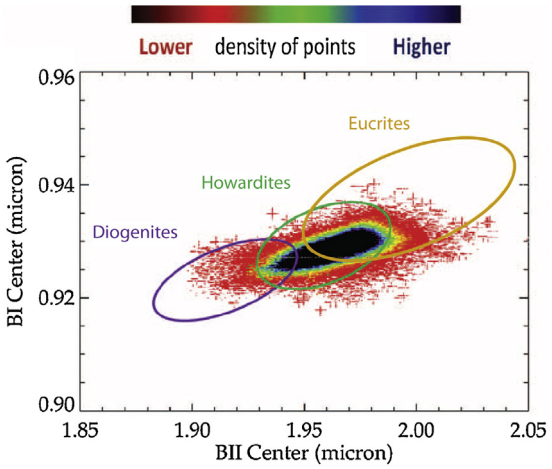

Fig. 10. BI vs. BII center of the vestan surface, relative to known HED BI and BII centers, as observed during Dawn's Survey mapping phase. Reprinted with permission from De Sanctis et al. (2012) Science 336: 697–700.

Upon approach to Vesta, VIR observed the surface in a spatial resolution twice that of HST and confirmed a dominance of BI and BII features that had been previously suggested (McCord et al., 1970). Higher spatial resolution analyses (~700 m/pixel) conducted by VIR during the Survey orbital stage revealed that a large portion of the surface of Vesta falls within the narrow 0.925–0.935 μm BI center and 1.93–1.99 μm BII center ranges, corresponding to howarditic compositions (Fig. 10). Similarly, at ~700 m/pixel, BI and BII depths for the majority of the surface match howardites, not pure eucritic or diogenitic end members (De Sanctis et al., 2012). Given that howardites are regolith breccias formed by impact mixing of diogenites and eucrites, it is not surprising that the surface is broadly howarditic, although they may not be entirely chemically or mineralogically representative of the present-day regolith. Several areas on the surface appear to be relatively more eucrite-, or diogenite-rich, though generally still "howardite" in composition. For example, the 505 km (diameter) Rheasilvia basin has BI and BII features that are stronger and centered at shorter wavelengths relative to the majority of the surface, as does a large swath of prospective ejecta material that dominates the eastern hemisphere (BII center shown in Fig. 11). These absorption features suggest that these areas are howarditic, but have higher concentrations of diogenitic material relative to the rest of the surface (De Sanctis et al., 2012). Reddy et al. (2012) highlighted these same features in FC images of the ratio of the 0.92 μm to 0.75 μm filters, a ratio that highlights the depth of the Band I feature, and the 0.98 μm to 0.92 μm ratio, which serves as a qualitative indicator of diogenite abundance. HED meteorite studies universally predict that diogenitic material would comprise lower crustal/upper mantle material, and thus support the observations made by VIR that the deepest crater on Vesta and its ejecta (Rheasilvia) contains the highest concentrations of diogenitic material. It is important to note that GRaND supports the general description of the surface as seen by VIR and FC during Survey orbit outlined above; the vestan surface is broadly howarditic with some regions appearing slightly more diogenitic or eucritic (Prettyman et al., 2013; Yamashita et al., 2013b; Lawrence et al., 2013; Peplowski et al., 2013). Reddy et al. (2013) compared Dawn, Hubble Space Telescope, and ground-based spectroscopy. These authors found reasonable to excellent agreement between these data sets for color and albedo and concluded that Dawn observations supported previous pre-Dawn observation of east–west dichotomy, the suggestion of exogenous carbonaceous chondritic material, and the dominance of diogenitic material in the eastern hemisphere, with most differences resulting from the much lower spatial resolution of ground-based and HST observations. A significant difference is in the interpretation of units argued to be olivine-rich by Gaffey (1997) and Binzel et al. (1997), which Le Corre et al. (2013) argue is likely impact melt and not olivine-rich on the basis of Dawn data. Upon descending into lower orbital altitudes, higher spatial resolution analyses by VIR (~200 m/pixel) revealed a few rare, discrete, seemingly igneous terrains. Using BI and BII center locations, Ammannito et al. (2013a) confirmed the presence of two small terrains at the base of the Rheasilvia central uplift and on a scarp of the Rheasilvia Basin called Matronalia Rupes (Fig. 12) that fall within the diogenite-rich end of the range of band centers for HED meteorites. These areas were previously postulated as pure diogenitic lithologies through the use of FC analysis of the BI feature (Reddy et al., 2012a,b; McSween et al., 2013a). In contrast, pure basaltic eucrite terrains are more difficult to establish using VIR due to overlaps in band centers with howardite compositions. However, the most eucrite-rich portion of the surface can be found near the equator (e.g., Reddy et al., 2012a,b; De Sanctis et al., 2012; Ammannito et al., 2013a; Prettyman et al., 2013), and corresponds

to most heavily cratered, oldest terrains on Vesta (Marchi et al., 2012). This suggests that the initial vestan upper crust was nearly pure eucrite, a hypothesis supported by HED meteorites.

Surprisingly, reflectance, gamma ray and neutron spectral data thus far show no signs of olivine in the Rheasilvia basin (McSween et al., 2013a; Prettyman et al., 2013; Ammannito et al., 2013a). Given the size of the Rheasilvia basin, it was anticipated that the mantle of Vesta would be exposed, likely including olivine-rich materials. Clenet et al. (2014) have suggested that the crust of Vesta is significantly thicker than suggested by models of HED petrogenesis. These authors suggest an ~80 km thick crust composed of eucritic crust with diogenitic intrusions, including the olivine-rich harzburgites. Alternatively, Toplis et al. (2013) calculate that olivine might comprise 60–70% of the mantle of Vesta, if it was derived from an H chondrite or H-CM chondrite mixture. This might suggest that dunitic rocks are rare in the mantle of Vesta. However, olivine-bearing rocks are known among the HED suite and it is instructive to consider their depth of formation and likely detection on the surface of Vesta. The olivine-rich harzburgites, or "olivine diogenites", known from the HED meteorites (Sack et al., 1991; Beck and McSween, 2010; Shearer et al., 2010) are predicted to form at depths equal to or less than those exposed by the Rheasilvia impact basin (McSween et al., 2013a), which sampled down to at least 30–45 km (Jutzi and Asphaug, 2011; Ivanov and Melosh, 2012) and possibly as deep as 50–70 km (Jutzi and Ivanov, 2014), and therefore based on HED studies, vestan harzburgites should be present in Rheasilvia. However, a study of unbrecciated harzburgitic HED meteorites suggests that the olivine abundance in pristine outcrops of harzburgitic material on Vesta might be too low (≤25%) to sufficiently distinguish the olivine-rich unit from the orthopyroxene-rich surrounding terrain using spectral reflectance (Beck et al., 2013). This, coupled with dilution via impact of the already low olivine abundances, suggests that olivine may be present in the Rheasilvia basin but currently unresolvable by Dawn.

In the northern hemisphere of Vesta, far away from areas enriched in diogenite, small patches with very high inferred abundances of olivine (>50%) have been observed (Ammannito et al., 2013b), although subsequent impact mixing and downslope movement obscure the exact scale of the olivine-rich areas. The areas in which these outcrops occur are generally eucrite-rich howardite and at very shallow depths at the walls of small impact craters. The location of this olivine-rich material appears to preclude sampling of exposed in situ mantle. Ammannito et al. (2013b) suggested that this material represents ejected olivine-rich (dunitic) mantle blocks. Cheek and Sunshine (2014) suggest that this material, which bears a Cr^{3+} spectral feature indicative of primitive melts, may represent a near-surface primitive lithology, possibly an indication of late stage serial magmatism. Petrologic and spectral data presented by Beck et al. (2014) suggest that the olivine-rich unit in the northern latitudes of Vesta may be akin to olivine-rich impact melts observed in some howardites.

5.2. GRaND observations of Vesta: Water and the unexpected

5.2.1. Hydrogen on Vesta

Neutron and gamma ray spectra acquired by GRaND were analyzed to determine the elemental composition of Vesta's regolith (Prettyman et al., 2012, 2013; Yamashita et al., 2013b; Lawrence et al., 2013; Peplowski et al., 2013). Perhaps one of the most interesting findings from the Dawn mission came from measurements of Vesta's neutron leakage spectrum. Neutrons are produced by the interaction of galactic cosmic rays (GCRs) with nuclei in the regolith. GCRs are ionized nucleons, primarily protons, with kinetic energies far in excess of the binding energy of atomic nuclei. GCR collisions break apart nuclei, producing a spray of secondary particles, including neutrons, which undergo successive collisions. Those that do not escape into space ultimately approach thermal equilibrium with the regolith, where they are lost by neutron capture. The leakage flux of epithermal neutrons (with kinetic energies roughly between 0.5 eV and 1 MeV) is highly sensitive to the concentration of H in the regolith. This has to do with the fact that neutrons have about the same mass as a hydrogen nucleus (proton). As in a game of billiards, a neutron will stop dead when it undergoes a head-on elastic collision with a proton; whereas, for heavier nuclei, only a portion of the neutron's kinetic energy will be lost. Neutrons primarily undergo "billiard-ball" collisions in the epithermal energy range. Thus, variations in the leakage flux of epithermal neutrons are caused primarily by changes in the concentration of H. Elastic scattering is also important for neutrons with higher energies; however, other processes result in reduced sensitivity for fast neutrons to H. GRaND measures leakage neutrons in the epithermal and fast energy ranges using a boron-loaded plastic scintillator, shielded from thermal neutrons (Prettyman et al., 2011, 2012, 2013). Maps of epithermal neutron counting rates were analyzed to determine the distribution and dynamic range of hydrogen on Vesta. We note that other volatiles key to the interpretation of a volatile-poor Vesta (e.g., Na and K) could not be measured by Dawn.

Geochemistry of the HED meteorites has led to the understanding that Vesta accreted from volatile poor material (McSween et al., 2011). Thus, it was not anticipated that endogenic H would be in high abundance on the vestan surface, and if present would likely be from an exogenic (foreign) source (Prettyman et al., 2011). GRaND measurements of epithermal neutron flux demonstrate that some areas in the regolith contain relatively high concentrations of H, with a range of 400 ppm (Fig. 13, top; Prettyman et al., 2012). The vestan fast neutron flux measured by GRaND supports the H concentrations derived from epithermal neutrons (Lawrence et al., 2013).

As described in Prettyman et al. (2012), H-rich areas on the surface of Vesta are also distinct in two other surface properties—albedo and age. H-rich areas are darker relative to the average surface albedo on Vesta (Fig 13, bottom). H-rich areas are also found within the oldest terrains on Vesta (Marchi et al., 2012). No endogenic, H-rich material in the HEDs can be evoked to explain the dark, old, H-rich areas observed on Vesta. However, two exogenic sources of H are possible: H implanted via solar wind, and incorporation of H-rich, exogenic carbonaceous chondrite material into the regolith via impact (Prettyman et al., 2012). While both implantation of solar wind and exogenic contamination would be more abundant in older terrains, incorporation of dark carbonaceous material would presumably have a much greater effect on surface albedo than implantation of solar wind. Further, if H on Vesta was from solar wind, the GRaND measurements would imply abundances that are ~4× greater than solar wind-implanted H on the Moon (Moon = ≤116 ppm solar wind H; Bustin and Gibson, 1992). Given the greater heliocentric distance of Vesta relative to the Moon, solar wind-implanted H should be lower on Vesta relative to the Moon, not greater. Through comparison of howardites with lunar soils and regolith breccias, Prettyman et al. (2012) inferred that the solar wind contribution to H in the vestan regolith is <100 ppm, and likely only a few ppm.

Perhaps the most compelling piece of evidence supporting a carbonaceous chondrite in-mixing origin for H on Vesta comes from the HED meteorites, where numerous studies have noted sizeable proportions of the HEDs containing carbonaceous chondrite fragments (e.g., ~10% of HEDs examined by Zolensky et al., 1996; ~12% of HEDs examined by Beck and McCoy, 2012). Using the range of carbonaceous chondrite modal abundances reported in HED breccias, and the average H concentration of a carbonaceous chondrite, Prettyman et al. (2012) estimated a range of ~240–600 ppm H in

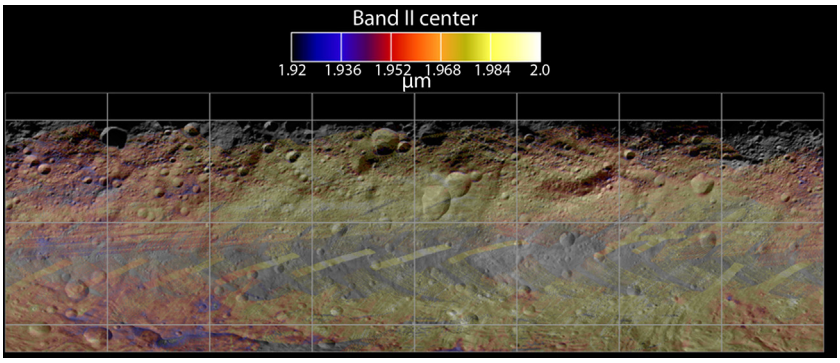

Fig. 11. Distribution of BII centers on the vestan surface, taken during Dawn's Survey mapping phase. Image courtesy of NASA/JPL-Caltech/UCLA/MPS/DLR/IDA.

HEDs containing exogenic carbonaceous chondrite material. This closely matches the range of H abundances in H-rich areas on the surface of Vesta, and strongly supports the hypothesis that H on the surface of Vesta is from the in-mixing of exogenic carbonaceous chondrite material. The dark material on Vesta was detected by Framing Camera clear and albedo images. FC data albedo vs. pyroxene band depth plot supported the interpretation that the dark material is an admixture of exogenic carbonaceous chondrite impactors and howardite regolith (Reddy et al., 2012a,b; Nathues et al., 2014). The VIR instrument also supports a carbonaceous chondrite source for the H-rich, dark areas on Vesta; a correlation was observed between a 2.8-μm absorption feature, commonly attributed to OH, and surface darkness (De Sanctis et al., 2012; McCord et al., 2012).

Given the correlation observed between H abundance and surface age on Vesta, carbonaceous chondrite in-mixing presumably occurred over a large span of time and not from one, or a few, impact events. This is supported by the petrology of carbonaceous material in the HEDs, where multiple sub-lithologies of carbonaceous chondrites have been identified (CM, CR, CV chondrites; Zolensky et al., 1996). However, alternative hypotheses evoking a single, giant CM2 chondrite impactor have been proposed as a possible source for much of the H-rich, dark material on Vesta (e.g., Reddy et al., 2012a,b); however, both large and small impacts must have contributed the observed material (Turrini et al., 2014). Because igneous activity on Vesta ceased shortly after formation of the asteroid (McSween et al., 2011), it has not subsequently undergone internally generated resurfacing, and thus retains a record of impact bombardment after initial differentiation. Other planetary bodies that had extended periods of geological evolution (the Moon, Mars) or are still geologically active (Earth) have had their early records of impact bombardment erased. Interestingly, the majority of chondritic asteroids have surface ages that are young (relative to Vesta) as well (Blitz et al., 2009). Though the timing of nebular condensation and formation of chondritic asteroids predates vestan differentiation, the surface age of most of those bodies was reset by the relatively recent family forming, collisional events (Bendjoya and Zappalå, 2002). Thus, Vesta is unique in that it is one of the few bodies that retain a surface record of impact bombardment from the early Solar System. It is presumable that exogenic, carbonaceous chondrite in-mixing was an important delivery process of H and other volatiles on other inner-Solar System bodies, evidence of which has been erased through subsequent resurfacing.

5.2.2. HED compositions on the surface

Data from the GRaND instrument also demonstrates a vestan surface that is largely howarditic in composition. To illustrate that here, we compare Fe concentrations and macroscopic thermal neutron absorption cross section (Σ_{eff}) measurements made by GRaND to those in HED meteorites. Gamma rays measured by GRaND's bismuth germinate sensor during Dawn's LAMO mapping phase were used to determine Fe concentrations on the surface. Those data were presented and discussed in Yamashita et al. (2013b), and the data shown in this work were taken from the NASA Planetary Data Systems (PDS) (Yamashita et al., 2013a). Vestan thermal neutron absorption data presented here also are from the NASA PDS (Prettyman, 2013), and were first presented and discussed in Prettyman et al. (2013). Fe concentrations and thermal neutron macroscopic absorption for cross sections for HEDs are part of a

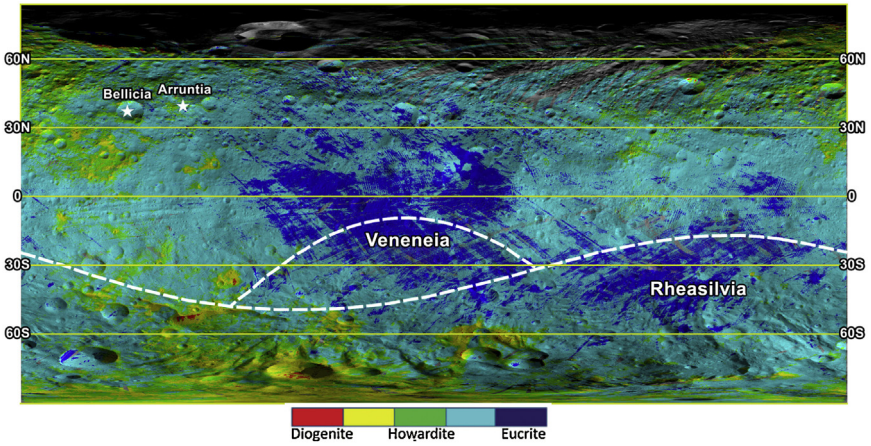

Fig. 12. Distribution of HED lithologies across the vestan surface, calculated from VIR data. Image courtesy of NASA/JPL-Caltech/UCLA/MPS/DLR/IDA, key was added based on a similar figure appearing in Ammannito et al. (2013a).

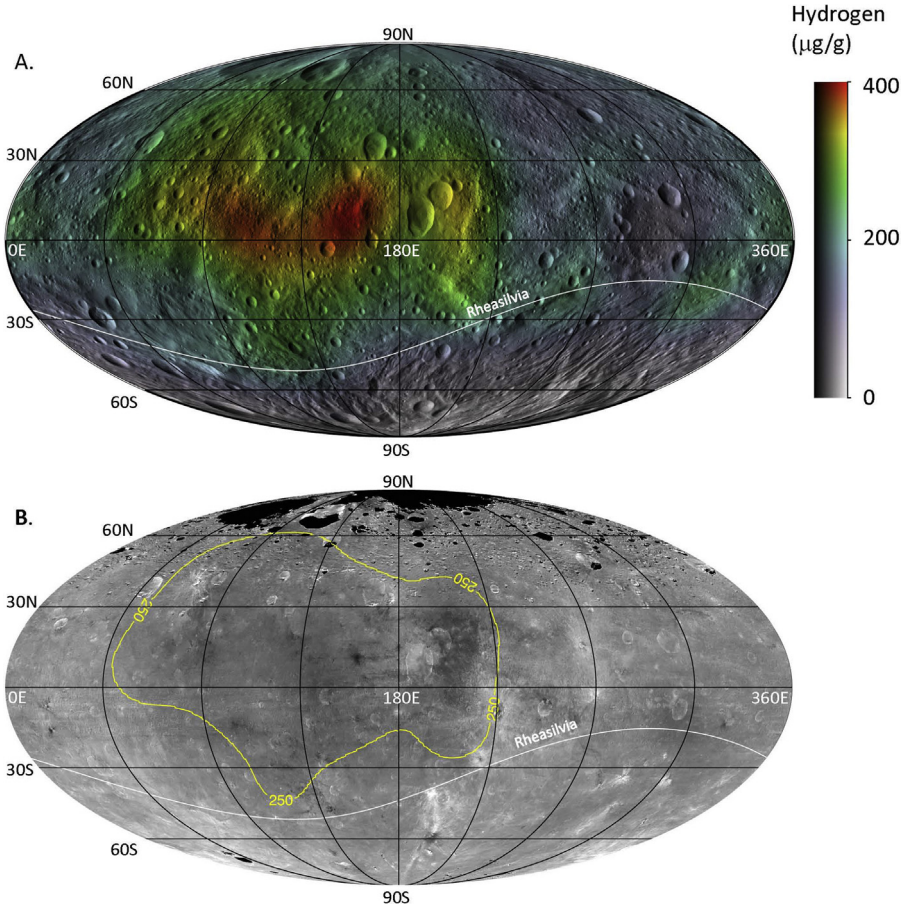

Fig. 13. A Mollweide projection map showing hydrogen abundances (Prettyman et al., 2012) on the surface of Vesta superimposed on shaded relief (top) and a HAMO 1 and 2 photometric-corrected mosaic showing albedo variation on the surface, overlain with a yellow contour denoting areas with ≥250 ppm hydrogen (bottom). The Rheasiliva crater rim is identified with a white line on both maps. (For interpretation of the references to color in this figure legend, the reader is referred to the web version of this article.)

dataset compiled by one of us (AWB), which are described in more detail in the caption of Fig. 14.

As can be seen in Fig. 14, basaltic eucrite, cumulate eucrite and orthopyroxenitic diogenites (the three main vestan igneous lithologies, as per the HEDs) establish three distinct regions in Fe vs. Σ_{eff}-space. Other, less common vestan igneous lithologies (e.g., Yamato Type B diogenite, harzburgite, dunite, Mg-rich diogenite) and exogenic material hypothesized to occur on Vesta (CM chondrite), are also shown. These units are all end members that, when brecciated and mixed in various proportions, create howardite. Not surprisingly, the howardite meteorites populate an area largely in between the three main vestan igneous lithologies in Fe vs. Σ_{eff}-space, though exceptionally CM- and olivine-rich[1] howardites would plot along tie-lines to those end members (Fig. 14).

As described previously, it is widely accepted that after differentiation ceased, Vesta had a basaltic eucrite veneer with cumulate eucrite and orthopyroxenitic diogenite emplaced at varied depths, with unit thickness, depth of emplacement and uniformity varying between differentiation models (McSween et al., 2011). It was presumed that through impacts, all of these end member lithologies would be exposed and could be mapped by Dawn to test differentiation models. However, as with BI and BII parameters measured by VIR (discussed in a previous section), the surface of Vesta appears largely howarditic in Fe vs. Σ_{eff} data measured by GRaND (dashed box, Fig. 14). GRaND measurements of Fe/Si vs. Fe/O show a similar howarditic composition for the majority of the surface (Prettyman et al., 2012). Measurements by GRaND do identify some areas of the vestan surface that appear to be more eucrite- or diogenite-rich howardite, but most are not "pure" compositions of these igneous end members. For example, Fe abundances (Yamashita et al., 2013b), neutron absorption (Prettyman et al., 2013), high-energy gamma rays (Peplowski et al., 2013) and fast neutron flux (Lawrence et al., 2013) all confirm that the Rheasilvia Basin and its ejecta are diogenite-rich; however, the variation is within the range of howardites and polymict breccias. Similarly, these data sets generally yield a howarditic composition that is more eucrite-rich in regions of the surface that are old and highly cratered. However, Peplowski et al. (2013) do identify several smaller areas within the highly-cratered equatorial terrain that have a high-energy gamma ray signature that matches basaltic and polymict eucrite exclusively, but not howardite.

The observations that more diogenite-rich howardite material correspond to large impact craters, and that eucrite-rich howardite material occurs in older terrains, allows the confirmation of general hypotheses about the petrogenesis of HEDs; diogenites formed deep beneath the surface of Vesta and the vestan upper crust was basaltic eucrite. However, the apparent lack of exposure of pure igneous units on every spatial scale sampled by Dawn would

[1] Beck et al. (2012b) report that Pecora Escarpment (PCA) 02015, 5 contains 7 vol.% olivine and 28 vol.% "olivine-rich impact melt", which in turn contains ~15–50 vol.% olivine. If the range of olivine in the impact melt is included in the total mode, olivine abundance in PCA 02015 is in the 11–21 vol.% range. The Fe/Σ_{eff} values and VISNIR spectra of that sample (Fig. 14 and Beck et al., 2014, respectively) support a high olivine concentration.

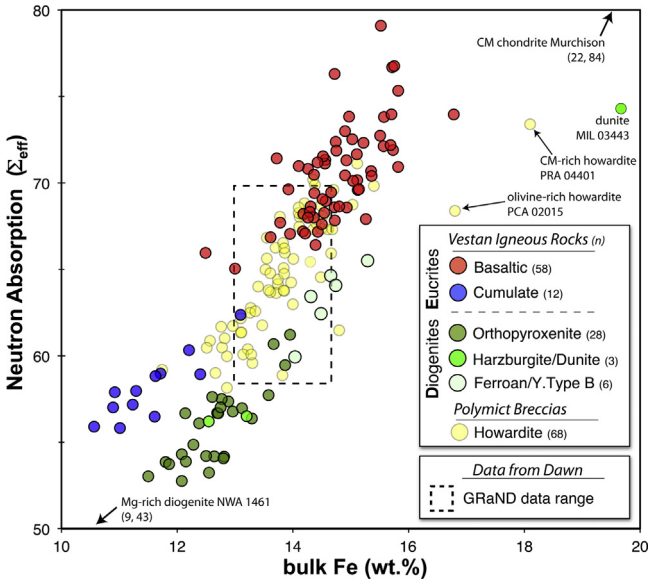

Fig. 14. Data points represent Fe concentrations and calculated effective macroscopic neutron absorption cross section (Σ_{eff}) of ~175 meteorites representing vestan igneous lithologies, polymict mixtures, and other end-member lithologies hypothesized to be present on Vesta. For clarity, "polymict eucrites" were not included; they roughly overlap the region between basaltic eucrites and howardites. All meteorite data contain ≥8 of the top 12 elements that contribute to Σ_{eff} in HEDs, as noted in Prettyman et al. (2013), the equations used to calculate meteorite Σ_{eff} can also be found in that reference. A box representing the range of GRaND-derived Fe concentrations and Σ_{eff} for the surface of Vesta overlies the meteorite data. Average Σ_{eff} uncertainty for Vesta data (±1.06) is not shown. Vesta Σ_{eff} and Fe concentration data come from the NASA Planetary Data System datasets Prettyman (2013) and Yamashita et al. (2013a), respectively. The majority of meteorite data are averages of multiple bulk element analyses and part of a dataset compiled by AWB. More than 120 references were used in that dataset, only some of which are listed here; references for the identified meteorites are: Murchison (Wilk, 1956; Jarosewich, 1971; Friedrich et al., 2002), Miller Range (MIL) 03443 (Beck et al., 2011), Mt. Pratt (PRA) 04401 (Mittlefehldt et al., 2013), PCA 02015 (Beck et al., 2012), and Northwest Africa (NWA) 1461 (Warren et al., 2009; Barrat et al., 2010; Schiller et al., 2011).

seem to suggest that questions regarding fine-scale structure of Vesta's crust (e.g., Shearer et al., 2010) remain unanswered. Perhaps the idea that distinct igneous terrains would be preserved well enough to answer such questions after 4.56 Ga of impact history and no igneous resurfacing was presumptuous. However, observations made by Dawn did further our understanding of regolith development on small bodies and identify a potentially important source of volatile delivery in the inner-Solar System.

6. The Vesta-HED connection

It was hoped that Dawn's mission to Vesta could both test the link between the howardite, eucrite, and diogenite meteorites and Vesta, and use inferences from petrologic and geochemical studies of these meteorites to guide our interpretation of the smallest, intact differentiated Solar System body. McSween et al. (2013b) present the lines of evidence from the mission that strengthen the link between Vesta and the HED meteorites. Among the most compelling of these are the general similarity in spectral features and bulk composition between Vesta and the howardites, the inferred age of the Rheasilvia basin and similarity to inferred ages for the meteorite-delivering vestoids, the presence of hydrogen in the regolith of Vesta consistent with inferred abundances of xenolithic carbonaceous chondrites in fragmental and regolithic howardites, and the constrained size of the core of Vesta consistent with geochemical models for differentiation of the HED parent body.

It is worth noting that while all of these indicators strengthen the link between HED meteorites and Vesta, they do not provide definitive proof of a connection. In the last decade, the unique link between HED meteorites and Vesta – first established when HED's included the known basaltic meteorites and Vesta was the only asteroid known to have a basaltic surface – has become muddled. As pointed out by Wasson (2013), iron meteorite evidence points to at least 26 asteroids that experienced extensive differentiation and likely formed a basaltic crust. Among these, oxygen isotopic compositions of HED meteorites and IIIAB irons are essentially identical. Oxygen isotopic compositions of basaltic meteorites have revealed a number of meteorites with anomalous $\Delta^{17}O$ compositions (Scott et al., 2009) which likely originated on separate parent bodies from the majority of the eucrites. Likewise, visible-near infrared spectroscopy has revealed asteroids with basaltic surfaces outside the population of vestoids, including 1459Magnya (Lazzaro et al., 2000), the Merxia and Agnia families and (17) Thetis (Sunshine et al., 2004). The semi-major axis of (17) Thetis is at the same heliocentric distance as the 3:1 meteorite-delivering resonance, although Thetis is nearly an order of magnitude larger than any of the impact-ejected vestoids. In the absence of direct sample return from Vesta, it is difficult to establish a conclusive link with the HED's, although the overwhelming body of evidence suggests that Vesta is the parent asteroid for these meteorites. One interesting possibility is that the older basins on Vesta, including Veneneia, also liberated asteroids which after 2 Ga of orbital evolution are no longer dynamically linked to Vesta.

A more interesting question is whether Dawn answered one of the driving questions behind exploring this smallest, intact differentiated world. Dawn achieved all of its Level 1 science objectives at Vesta (Russell et al., 2013), but it left largely unanswered the question of whether Vesta differentiated via a magma ocean or serial magmatism or a combination of the two. While the megaregolith of Vesta was largely homogenized by impact bombardment, the predominance of diogenite-rich howardite in the Rheasilvia basin is consistent with a thick layer of diogenitic material underlying eucritic material. As pointed out by McSween et al. (2013b), this alone does not provide unambiguous support for either a magma ocean model (Righter and Drake, 1997; Ruzicka et al., 1997) or serial magmatism (Mittlefehldt, 1994; Beck and McSween, 2010), both of which predict diogenitic material underlying eucrites. While the idea of a magma ocean was first championed for the Moon (Wood et al., 1970) and has been subsequently been widely adopted for a number of Solar System bodies, our exploration of Vesta failed to provide definitive evidence of an early magma ocean, leaving open to question the primary mechanism by which most planetary bodies differentiated.

7. The future

Dawn is currently in route to asteroid (1) Ceres with scheduled arrival in early 2015. At Ceres, Dawn should provide new insights into a fundamentally different style of planetary differentiation. Rather than the high-temperature metal–silicate differentiation that dominated the early history of the inner Solar System, Ceres likely records early ice-rock differentiation of a style far more common in the satellites of the outer Solar System. From this perspective, Dawn should serve to bookend the two major styles of planetary differentiation.

An equally compelling question is the next logical step in understanding high-temperature metal–silicate differentiation. Typically, the eventual goal of planetary exploration after remote exploration is sample return. In the case of (4) Vesta, a sample return mission may not be the next logical step. Although detailed laboratory study and analysis of data acquired by Dawn may eventually provide conclusive evidence for or against a Vesta-HED link, a random sample of the regolith of Vesta is unlikely to significantly

advance our understanding of this asteroid. Indeed, Vesta is, by mass, the best sampled planetary body aside from Earth if HEDs do hail from there. Instead, the next logical step in understanding this style of differentiation might be a mission that bookends not a different style, but a different location of differentiation. Metallic asteroids can offer the possibility of examining the stripped core of a differentiated asteroid, possibly sampling the core-mantle boundary. An orbital, remote-sensing mission could provide unique insights into the nature of the lower mantle, the transition from the core to the mantle, and the structure of the core, including incorporation of light elements like sulfur, carbon, or silicon. Among possible targets, asteroid (16) Psyche, at some 200 km in diameter, may provide the best target for such a mission.

Acknowledgments

We thank the entire Dawn engineering and science teams, without whom this mission would not have succeeded. We thank the NASA Dawn at Vesta Participating Scientist Program for funding for this work and Associate Editor Dr. Klaus Keil for inviting submission of this paper. Reviews by Vishnu Reddy, Jessica Sunshine and an anonymous reviewer significantly improved the manuscript. A portion of this work was carried out by the Planetary Science Institute under contract with the NASA Jet Propulsion Laboratory.

References

Ammannito, E., De Sanctis, M.C., Capaccioni, F., Capria, M.T., Carraro, F., Combe, J.-P., Fonte, S., Frigeri, A., Joy, S., Longobardo, A., Magni, G., Marchi, S., McCord, T., McFadden, L., McSween, H., Palomba, E., Pieters, C., Polanskey, C., Raymond, C., Sunshine, J., Tosi, F., Zambon, F., Russell, C., 2013a. Vestan lithologies mapped by the visual and infrared spectrometer on Dawn. Meteorit. Planet. Sci. 48, 2185–2198.

Ammannito, E., De Sanctis, M., Palomba, E., Longobardo, A., Mittlefehldt, D., McSween, H., Marchi, S., Capria, M., Capaccioni, F., Frigeri, A., Pieters, C., Ruesch, O., Tosi, F., Zambon, F., Carraro, F., Fonte, S., Giesinger, H., Magni, G., McFadden, L., Raymond, C., Russell, C., Sunshine, J., 2013b. Olivine in an unexpected location on Vesta's surface. Nature 504, 122–125.

Barrat, J., Yamaguchi, A., Zanda, B., Bollinger, C., Bohn, M., 2010. Relative chronology of crust formation on asteroid Vesta: insights from the geochemistry of diogenites. Geochim. Cosmochim. Acta 74, 6218–6231.

Beck, A., McSween, H., 2010. Diogenites as polymict breccias composed of harzburgitic and orthopyroxenitic lithologies. Meteorit. Planet. Sci. 45, 850–872.

Beck, A., Mittlefehldt, D., McSween, H., Rumble, D., Lee, C.-T.A., Bodnar, R., 2011. MIL 03443, a dunite from asteroid 4 Vesta: evidence for its classification and cumulate origin. Meteorit. Planet. Sci. 46, 1133–1151.

Beck, A., McCoy, T., 2012. Dark material in HED and OC breccias: implications for asteroid surfaces (abstract). In: 75th Annual Meteoritical Society Meeting, Abstract #5328.

Beck, A., Welten, K., McSween, H., Viviano-Beck, C., Caffee, M., 2012. Petrologic and textural diversity among the PCA 02 Howardite group, one of the largest pieces of the vestan surface. Meteorit. Planet. Sci. 47, 947–969.

Beck, A., McCoy, T., Sunshine, J., Viviano, C., Corrigan, C., Hiroi, T., Mayne, R., 2013. Challenges in detecting olivine on the surface of 4 Vesta. Meteorit. Planet. Sci. 48, 2155–2165.

Beck, A., Lunning, N., De Sanctis, M., Hiroi, T., Plescia, J., Viviano-Beck, C., Udry, A., Corrigan, C., McCoy, T., 2014. A meteorite analog for olivine-rich terrain in unexpected locations on Vesta. In: 45th Lunar and Planetary Science Conference Abstract #2499.

Bendjoya, P., Zappalà, V., 2002. Asteroid family identification. In: Bottke, W., Cellino, A., Paolicchi, P., Binzel, P.R. (Eds.), Asteroids III. The University of Arizona Press, Tucson, AZ, pp. 613–618.

Binzel, R.P., Xu, S., 1993. Chips off of asteroid 4 Vesta: evidence for the parent body of basaltic achondrite meteorites. Science 260, 186–191.

Binzel, R.P., Gaffey, M.J., Thomas, P.T., Zellner, B.H., Storrs, A.D., Wells, E.N., 1997. Geologic mapping of Vesta from 1994 Hubble Space Telescope images. Icarus 128, 95–103.

Blitz, C., Lognonné, P., Komatitsch, D., Baratoux, D., 2009. Effects of ejecta accumulation on the crater population of asteroid 433 Eros. J. Geophys. Res. 114, E06006.

Bobrovnikoff, N.T., 1929. The spectra of minor planets. Lick Obs. Bull. 407, 18–27.

Brophy, J., 2011. The Dawn ion propulsion system. Space Sci. Rev. 163, 251–261.

Buczkowski, D.L., Wyrick, D.Y., Iyer, K.A., Kahn, E.G., Scully, J.E.C., Nathues, A., Gaskell, R.W., Roatsch, T., Preusker, F., Schenk, P.M., Le Corre, L., Reddy, V., Yingst, R.A., Mest, S., Williams, D.A., Garry, W.B., Barnouin, O.S., Jaumann, R., Raymond, C.A., Russell, C.T., 2012. Large-scale troughs on Vesta: a signature of planetary tectonics. Geophys. Res. Lett. 39, L18205.

Burns, R.G., 1993. Origin of electronic spectra of minerals in the visible-near infrared region. In: Pieters, C., Englert, P. (Eds.), Remote Geochemical Analysis: Elemental Mineralogical Compositions. Cambridge Univ. Press, Cambridge, UK, pp. 3–29.

Bustin, R., Gibson, E., 1992. Availability of hydrogen for lunar base activities. In: Mendell, W. (Ed.), The Second Conference on Lunar Bases and Space Activities of the 21st Century. NASA, Washington, DC, pp. 437–445.

Cheek, L.C., Sunshine, J.M., 2014. Spectral mixture analysis as a tool for characterizing the distribution of Vesta's olivine-rich material. In: 45th Lunar and Planetary Science Conference #2735.

Clenet, H., Jutzi, M., Barrat, J.-A., Asphaug, E.I., Benz, W., Gillet, P., 2014. A deep crust-mantle boundary in the asteroid 4 Vesta. Nature 511, 303–306.

Consolmagno, G.J., Britt, D.T., Macke, R.J., 1998. The significance of meteorite density and porosity. Chem. Erde—Geochem. 68, 1–29.

Corrigan, C.M., Welzenbach, L.C., Righter, K., McBride, K., McCoy, T.J., Harvey, R.P., Satterwhite, C., 2014. A statistical look at the US Antarctic meteorite collection. In: Righter, K., Harvey, R., Corrigan, C.M., McCoy, T.J. (Eds.), 35 Seasons of U.S. Antarctic Meteorites (1976–2010): A Pictorial Guide to the Collection. AGU-Wiley Press, Hoboken, NJ, USA, pp. 173–187.

De Sanctis, M.C., Cordiani, A., Ammannito, E., Filacchione, G., Capria, M.T., Fonte, S., Magni, G., Barbis, A., Bini, A., Dami, M., Ficai-Veltroni, I., Preti, G., VIR Team, 2011. The VIR spectrometer. Space Sci. Rev. 163, 329–369.

De Sanctis, M.C., Ammannito, E., Capria, M.T., Tosi, F., Capaccioni, F., Zambon, F., Carraro, F., Fonte, S., Frigeri, A., Jaumann, R., Magni, G., Marchi, S., McCord, T., McFadden, L., McSween, H., Mittlefehldt, D., Nathues, A., Palomba, E., Pieters, C., Raymond, C., Russell, C., Toplis, M., Turrini, T., 2012. Spectroscopic characterization of mineralogy and its diversity across Vesta. Science 336, 697–700.

Friedrich, J., Wang, M.-S., Lipschutz, M., 2002. Comparison of the trace element composition of Tagish Lake with other primitive carbonaceous chondrites. Meteorit. Planet. Sci. 37, 677–686.

Gaffey, M., 1976. Spectral reflectance characteristics of the meteorite classes. J. Geophys. Res. 81, 905–920.

Gaffey, M.J., 1997. Surface lithologic heterogeneity of Asteroid 4 Vesta. Icarus 127, 130–157.

Hertz, H.G., 1968. Mass of Vesta. Science 160, 299–300.

Hughes, D.W., 1994. The historical unravelling of the diameters of the first four asteroids. Q. J. R. Astron. Soc. 35, 331.

Ivanov, B., Melosh, H., 2012. The Rheasilvia crater on Vesta: numerical modeling. In: Lunar and Planetary Science Conference 43, Abstract #2148.

Jarosewich, E., 1971. Chemical analysis of the Murchison meteorite. Meteoritics 6, 49–52.

Jaumann, R., Williams, D.A., Buczkowski, D.L., Yingst, R.A., Preusker, F., Hiesinger, H., Schmedemann, N., Kneissl, T., Vincent, J.B., Blewett, D.T., Buratti, B.J., Carsenty, U., Denevi, B.W., De Sanctis, M.C., Garry, W.B., Keller, H.U., Kersten, E., Krohn, K., Li, J.-Y., Marchi, S., Matz, K.D., McCord, T.B., McSween, H.Y., Mest, S.C., Mittlefehldt, D.W., Mottola, S., Nathues, A., Neukum, G., O'Brien, D.P., Pieters, C.M., Prettyman, T.H., Raymond, C.A., Roatsch, T., Russell, C.T., Schenk, P., Schmidt, B.E., Scholten, F., Stephan, K., Sykes, M.V., Tricarico, P., Wagner, R., Zuber, M.T., Sierks, H., 2012. Vesta's shape and morphology. Science 336, 687–690.

Jutzi, M., Asphaug, E., 2011. Mega-ejecta on asteroid Vesta. Geophys. Res. Lett. 38, L01102.

Jutzi, M., Ivanov, B.A., 2014. Modelling the Rheasilvia impact. In: Vesta in the Light of Dawn: First Exploration of a Protoplanet in the Asteroid Belt. Abstract #2008.

Lazzaro, D., Michtchenko, T., Harris, A.W., 2000. Discovery of a basaltic asteroid in the outer main belt. Science 288, 2033.

Lawrence, D., Peplowski, P., Prettyman, T., Feldman, W., Bazell, D., Mittlefheldt, D., Reedy, R., Yamashita, N., 2013. Constraints on Vesta's elemental composition: fast neutron measurements by Dawn's gamma ray and neutron detector. Meteorit. Planet. Sci. 48, 2271–2288.

Le Corre, L., Reddy, V., Schmedemann, N., Becker, K.J., O'Brien, D.P., Yamashita, N., Peplowski, P.N., Prettyman, T.H., Li, J.-Y., Cloutis, E.A., Denevi, B.W., Kneissl, T., Palmer, E., Gaskell, R.W., Nathues, A., Gaffey, M.J., Mittlefehldt, D.W., Garry, W.B., Sierks, H., Russell, C.T., Raymond, C.A., De Sanctis, M.C., Ammanito, E., 2013. Olivine or impact melt: nature of the "orange" material on Vesta from Dawn. Icarus 226, 1568–1594.

Marchi, S., McSween, H., O'Brien, D., Schenk, P., De Sanctis, M., Gaskell, R., Jaumann, R., Mottola, S., Preusker, F., Raymond, C., Russell, C., 2012. The violent collisional history of asteroid 4 Vesta. Science 336, 690–694.

Mason, B., 1962. Meteorites. John Wiley and Sons, Inc., New York, NY.

Mayne, R., Sunshine, J., McSween, H., McCoy, T., Corrigan, C., Gale, A., 2010. Insights from the spectra of unbrecciated eucrites: implications for Vesta and basaltic asteroids. Meteorit. Planet. Sci. 45, 1074–1092.

McCord, T.B., Adams, J.B., Johnson, T.V., 1970. Asteroid Vesta: spectral reflectivity and compositional implications. Science 168, 1445–1447.

McCord, T., Li, J.-Y., Combe, J.-P., McSween, H., Jaumann, R., Reddy, V., Tosi, F., Williams, D., Blewett, D., Turrini, D., Palomba, E., Pieters, C., De Sanctis, M., Ammannito, E., Capria, M., Le Corre, L., Longobardo, A., Nathues, A., Mittlefehldt, D., Schroder, S., Hiesinger, H., Beck, A., Capaccioni, F., Carsenty, U., Keller, H., Denevi, B., Sunshine, J., Raymond, C., Russell, C., 2012. Dark material on Vesta from the infall of carbonaceous volatile-rich material. Nature 491, 83–86.

McSween, H.Y., Mittlefehldt, D.W., Beck, A.W., McCoy, T.J., Mayne, R.G., 2011. HED meteorites and their relationship to the geology of Vesta and the Dawn Mission. Space Sci. Rev. 163, 141–174.

McSween, H., Ammannito, E., Reddy, V., Prettyman, T., Beck, A., De Sanctis, M., Nathues, A., Le Corre, L., O'Brien, D., Yamashita, N., McCoy, T., Mittlefehldt, D., Toplis, M., Schenk, P., Palomba, E., Turrini, D., Tosi, F., Zambon, F., Longobardo,

A., Capaccioni, F., Raymond, C., Russell, C., 2013a. Composition of the Rheasilvia basin, a window into Vesta's interior. J. Geophys. Res.: Planets 118, 335–346.
McSween Jr., H.Y., Binzel, R.P., De Sanctis, M.C., Ammannito, E., Prettyman, T.H., Beck, A.W., Reddy, V., Le Corre, L., Gaffey, M.J., McCord, T.B., Raymond, C.A., Russell, C.T., The Dawn Science Team, 2013b. Dawn; the Vesta-HED connection; and the geologic context for eucrites, diogenites, and howardites. Meteorit. Planet. Sci. 48, 2090–2104.
Mittlefehldt, D.W., 1994. The genesis of diogenites and HED parent body petrogenesis. Geochim. Cosmochim. Acta 58, 1537–1552.
Mittlefehldt, D.W., McCoy, T.J., Goodrich, C.A., Kracher, A., 1998. Non-chondritic meteorites from asteroidal bodies. In: Papike, J.J. (Ed.), Planetary Materials Reviews in Mineralogy, 36, 4-1-195.
Mittlefehldt, D., Herrin, J., Quinn, J., Mertzman, S., Cartwright, J., Mertzman, K., Peng, Z., 2013. Composition and petrology of HED polymict breccias: the regolith of (4) Vesta. Meteorit. Planet. Sci. 48, 2105–2134.
Nathues, A., Hoffmann, M., Cloutis, E., Schäfer, M., Reddy, V., Christensen, U., Sierks, H., Thangjam, G.S., Le Corre, L., Mengel, K., Vincent, J.B., Russel, C.T., Prettyman, T., Schmedemann, N., Kneissl, T., Raymond, C., Gutiérrez Marqués, P., Hall, I., Büttner, I., 2014. Detection of serpentine in exogenic carbonaceous chondrite material on Vesta from Dawn FC data. Icarus 239, 222–237.
Newsom, H.E., 1985. Molybdenum in eucrites: evidence for a metal core in the eucrite parent body. In: Proc. 15th Lunar Planet. Sci. Conf, pp. C613–C617.
O'Brien, D.P., Marchi, S., Morbidelli, A., Bottke, W.F., Schenk, P., Russell, C.T., Raymond, C.A., 2014. The impact history of Vesta. In: Vesta in the Light of Dawn: First exploration of a Protoplanet in the Asteroid Belt. Abstract #2049.
Ostro, S.J., Campbell, D.B., Pettengill, G.H., Shapiro, I.I., 1980. Radar detection of Vesta. Icarus 43, 169–171.
Peplowski, P., Lawrence, D., Prettyman, T., Yamashita, N., Bazell, D., Feldman, W., Le Corre, L., McCoy, T., Reddy, V., Reedy, R., Russell, C., Toplis, M., 2013. Compositional variability on the surface of 4 Vesta revealed through GRaND measurements of high-energy gamma rays. Meteorit. Planet. Sci. 48, 2105–2134.
Prettyman, T., 2013. Dawn GRaND Absorption Map, A-GRAND-5-VESTA-ABSROPTION-v1.0. NASA Planetary Data System.
Prettyman, T.H., Feldman, W.C., McSween Jr., H.Y., Dingler, R.D., Enemark, D.C., Patrick, D.E., Storms, S.A., Hendricks, J.S., Morgenthaler, J.P., Pitman, K.M., Reedy, R.C., 2011. Dawn's gamma ray and neutron detector. Space Sci. Rev. 163, 371–459.
Prettyman, T., Mittlefehldt, D., Yamashita, N., Lawrence, D., Beck, A., Feldman, W., McCoy, T., McSween, H., Toplis, M., Titus, T., Tricarico, P., Reedy, R., Hendricks, J., Forni, O., Le Corre, L., Li, J.-Y., Mizzon, H., Reddy, V., Raymond, C., Russell, C., 2012. Elemental mapping by Dawn reveals exogenic H in Vesta's regolith. Science 338, 242–246.
Prettyman, T., Mittlefehldt, D., Yamashita, N., Beck, A., Feldman, W., Hendricks, J., Lawrence, D., McCoy, T., McSween, H., Peplowski, P., Reedy, R., Toplis, M., Le Corre, L., Mizzon, H., Reddy, V., Titus, T., Raymond, C., Russell, C., 2013. Neutron absorption constraints on the composition of 4 Vesta. Meteorit. Planet. Sci. 48, 2211–2236.
Reddy, V., Li, J.-Y., Le Corre, L., Scully, J.E.C., Gaskell, R., Russell, C.T., Park, R.S., Nathues, A., Raymond, C., Gaffey, M.J., Sierks, H., Becker, K.J., McFadden, L.A., 2013. Comparing Dawn, Hubble Space Telescope, and ground-baed interpretation of (4) Vesta. Icarus 226, 1103–1114.
Reddy, V., Le Corre, L., O'Brien, D., Nathues, A., Cloutis, E., Durda, D., Bottke, W., Bhatt, M., Nesvorny, D., Buczkowski, D., Scully, J., Palmer, E., Sierks, H., Mann, P., Becker, K., Beck, A., Mittlefehldt, D., Li, J.-Y., Gaskell, R., Russell, C., Gaffey, M., McSween, H., McCord, T., Combe, J.-P., Blewett, D., 2012a. Delivery of dark material to Vesta to carbonaceous chondritic impacts. Icarus 221, 544–559.
Reddy, V., Nathues, A., Le Corre, L., Sierks, H., Li, J.-Y., Gaskell, R., McCoy, T., Beck, A., Schroder, S., Pieters, C., Becker, K., Buratti, B., Denevi, B., Blewett, D., Christensen, U., Gaffey, M., Marques-Gutierrez, P., Hicks, M., Keller, H., Maue, T., Mottola, S., McFadden, L., McSween, H., Mittlefehldt, D., O'Brien, D., Raymond, C., Russell, C., 2012b. Color and albedo heterogeneity of Vesta from Dawn. Science 336, 700–704.
Righter, K., Drake, M.J., 1997. A magma ocean on Vesta: core formation and petrogenesis of eucrites and diogenites. Meteorit. Planet. Sci. 32, 929–944.
Russell, C.T., Raymond, C.A., 2011. The Dawn mission to Vesta and Ceres. Space Sci. Rev. 163, 3–23.
Russell, C.T., Raymond, C.A., Cordiani, A., McSween, H.Y., Zuber, M.T., Nathues, A., De Sanctis, M.C., Jaumann, R., Konopliv, A.S., Preusker, F., Asmar, S.W., Park, R.S., Gaskell, R., Mottola, S., Roatsch, T., Scully, J.E.C., Smith, D.E., Tricarino, P., Toplis, M.J., Christensen, U.R., Feldman, W.C., Lawrence, D.J., McCoy, T., Prettyman, T.H., Reedy, R.C., Sykes, M.E., Titus, T.N., 2012. Dawn at Vesta: testing the protoplanetary paradigm. Science 336, 684–686.
Russell, C.T., Raymond, C.A., Jaumann, R., McSween, H.Y., De Sanctis, M.C., Nathues, A., Prettyman, T.H., Ammannito, E., Reddy, V., Preusker, F., O'Brien, D.P., Marchi, S., Denevi, B.W., Buczkowski, D.L., Pieters, C.M., McCord, T.B., Li, J.-Y., Mittlefehldt, D.W., Combe, J.-P., Williams, D.A., Hiesinger, H., Yingst, R.A., Polanskey, C.A., Joy, P., 2013. Dawn completes its mission at 4 Vesta. Meteorit. Planet. Sci. 48, 2076–2089.
Ruzicka, A., Snyder, G.A., Taylor, L.A., 1997. Vesta as the howardite, eucrite and diogenite parent body: implications for the size of the core and for large-scale differentiation. Meteorit. Planet. Sci. 32, 825–840.
Sack, R., Azeredo, W., Lipschutz, M., 1991. Olivine diogenites: the mantle of the eucrite parent body. Geochim. Cosmochim. Acta 55, 1111–1120.
Schenk, P., O'Brien, D.P., Marchi, S., Gaskell, R., Preusker, F., Roatsch, T., Jaumann, R., Buczkowski, D., McCord, T.B., McSween, H.Y., Williams, D., Yingst, A., Raymond, C., Russell, C., 2012. The geologically recent giant impact basins at Vesta's south pole. Science 336, 694–697.
Schiller, M., Baker, J., Creech, J., Paton, C., Millet, M.-A., Irving, A., Bizzarro, M., 2011. Rapid timescales for magma ocean crystallization on the howardite–eucrite–diogenite parent body. Astrophys. J. Lett. 740, L22.
Scott, E.R.D., Greenwood, R.C., Franchi, I.A., Sanders, I.S., 2009. Oxygen isotopic constraints on the origin and parent bodies of eucrites, diogenites, and howardites. Geochim. Cosmocim. Acta 73, 5835–5853.
Shearer, C., Burger, P., Papike, J., 2010. Relationships between diogenites and olivine diogenites: implications for magmatism on the HED parent body. Geochim. Cosmochim. Acta 74, 4865–4880.
Sierks, H., Keller, H.U., Jaumann, R., Michalik, H., Behnke, T., Bubenhagen, F., Büttner, I., Carsenty, U., Christensen, U., Enge, R., Fiethe, B., Gutiérrez Marqués, P., Hartwig, H., Krüger, H., Kühne, W., Maue, T., Mottola, S., Nathues, A., Reiche, K.-U., Richards, M.L., Roatsch, T., Schröder, S.E., Szemerey, I., Tschentscher, M., 2011. The Dawn framing camera. Space Sci. Rev. 163, 263–327.
Sunshine, J.M., Bus, S.J., McCoy, T.J., Burbine, T.H., Corrigan, C.M., Binzel, R.P., 2004. High-calcium pyroxene as an indicator of igneous differentiation in asteroids and meteorites. Meteorit. Planet. Sci. 39, 1343–1357.
Thomas, P.C., Binzel, R.P., Gaffey, M.J., Storrs, A.D., Wells, E.N., Zellner, B.H., 1997. Impact excavation on asteroid 4 Vesta: Hubble Space Telescope results. Science 277, 1492–1495.
Thomas, V.C., Makowski, J.M., Brown, G.M., McCarthy, J.F., Bruno, D., Cardoso, J.C., Chiville, W.M., Meyer, T.F., Nelson, K.E., Pavri, B.E., Termohlen, D.A., Violet, M.D., Williams, J.B., 2011. The Dawn spacecraft. Space Sci. Rev. 163, 175–249.
Toplis, M.J., Mizzon, H., Monnereau, M., Forni, O., McSween, H.Y., Mittlefehldt, D.W., McCoy, T.J., Prettyman, T.H., Sanctis, M.C., Raymond, C.A., Russell, C.T., 2013. Chondritic models of 4 Vesta: implications for geochemical and geophysical properties. Meteorit. Planet. Sci. 48, 2300–2315.
Turrini, D., Combe, J.-P., McCord, T.B., Oklay, N., Vincent, J.-B., Prettyman, T.H., McSween, H.Y., Consolmagno, G.J., De Sanctis, M.C., Le Corre, L., Longobardo, A., Palomba, E., Russell, C.T., 2014. The contamination of the surface of Vesta by impacts and the delivery of the dark material. Icarus, in press.
Wadhwa, M., Srinivasan, G., Carlson, R.W., 2006. Timescales of planetesimal differentiation in the early solar system. In: Lauretta, D.S., McSween Jr., H.Y. (Eds.), Meteorites and the Early Solar System II. Univ. of Arizona Press, Tucson, AZ, USA, pp. 715–731.
Warren, P., Kallemeyn, G., Hubner, H., Ulff-Moller, F., Choe, W., 2009. Siderophile and other geochemical constraints on mixing relationships among HED-meteoritic breccias. Geochim. Cosmochim. Acta 73, 5918–5943.
Wasson, J.T., 2013. Vesta and extensively melted asteroids: why HED meteorites are probably not from Vesta. Earth Planet. Sci. Lett. 381, 138–146.
Wilk, H., 1956. The chemical composition of some stony meteorites. Geochim. Cosmochim. Acta 9, 279–289.
Wood, J.A., Dickey Jr., J.S., Marvin, U.B., Powell, B.N., 1970. Lunar anorthosites. Science 167, 602.
Yamashita, N., Prettyman, T., Mittlefehldt, D., Toplis, M., McCoy, T., Beck, A., Reedy, R., Feldman, W., Lawrence, D., Peplowski, P., Forni, O., Mizzon, H., Raymond, C., Russell, C., 2013a. DAWN-A-GRAND-5-VESTA-GAMMA-IRON-COR-v1.0. NASA Planetary Data System.
Yamashita, N., Prettyman, T., Mittlefehldt, D., Toplis, M., McCoy, T., Beck, A., Reedy, R., Feldman, W., Lawrence, D., Peplowski, P., Forni, O., Mizzon, H., Raymond, C., Russell, C., 2013b. Distribution of iron on Vesta. Meteorit. Planet. Sci. 48, 2237–2251.
Zolensky, M., Weisberg, M., Buchanan, P., Mittlefehldt, D., 1996. Mineralogy of carbonaceous chondrite clasts in HED achondrites and the Moon. Meteorit. Planet. Sci. 31, 518–537.
Zuber, M.T., McSween Jr., H.Y., Binzel, R.P., Elkins-Tanton, L.T., Konopliv, A.S., Pieters, C.M., Smith, D.E., 2011. Origin, internal structure and evolution of 4 Vesta. Space Sci. Rev. 163, 77–93.